Wearable Hand Rehabilitation Robot Capable of Hand Function Assistance in Stroke Survivors*

Ju-Hwan Bae, Young-Min Kim and Inhyuk Moon, *Member, IEEE*

Abstract—In this paper, we propose DULEX-II, a wearable hand robot capable of assisting stroke survivors with hand function rehabilitation. DULEX-II is a robotic orthosis that has three degrees of freedom for assisting motions of the wrist, and all fingers, excluding the thumb. Each exoskeleton mechanism enclosing the wrist and fingers is designed to fit the user's motion trajectory. DULEX-II is actuated by three linear actuators: a double-acting pneumatic cylinder for the wrist and two electric linear motors for the fingers. All mechanisms were analyzed by kinematics, and then a control system for hand rehabilitation was designed. Using the experimental results obtained for self-motion control using a data-glove, we demonstrated that DULEX-II is capable of performing hand rehabilitation exercises similar to those performed in mirror therapy.

Fig. 1. Hand rehabilitation robot, DULEX-II.

I. INTRODUCTION

STROKE results in the loss of brain function due to disturbance in the blood supply to the brain by cerebrovascular accident (CVA). In recent years, stroke has been the leading cause of adult disability and the second or third cause of death in developing countries [1]. It causes functional disabilities in one or more of the limbs, or disturbances in sensory function. It is known that repetitive rehabilitation with a therapist is an effective method for improving motor-functional disabilities in stroke survivors. Specialized occupational therapy and functional exercises are also helpful in improving body function. Such rehabilitation therapy requires a great deal of physical labor on the part of occupational and physical therapists, as well as great expenditure in terms of money and time. Therefore, the demand for robotic rehabilitation devices to assume part of the role of the therapist has been increasing; several studies have already been conducted [2-3]. In recent years, there has been a great deal of research related to upper-limb rehabilitation robots to assist stroke survivors in the performance of rehabilitation exercise; a robot for shoulder and elbow rehabilitation [4]; and a hand rehabilitation robot [5] to enable patients to stretch and strengthen muscles. However, none of these studies addressed the need to perform
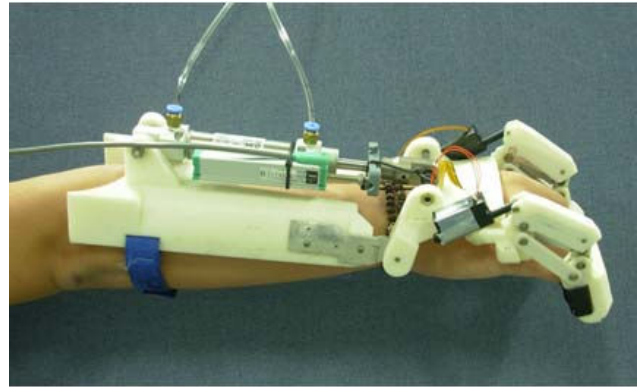
independent motion in the wrist and fingers. Subsequently, a robotic hand rehabilitation device with a multiple degree of freedom (DOF) was introduced. Ueki et al. [6] presented a hand rehabilitation robot with 16 DOF for the hand and 2 DOF for the wrist. In [7], a finger rehabilitation robot, not of the exoskeleton type, was introduced. These devices were useful for making human-like motions, but patients were required to visit a hospital equipped for rehabilitation exercise because most of the abovementioned equipment was fixed in a laboratory.

Recently, wearable robotic orthoses have been actively studied, according to the progress in robot technology. Robotic orthoses assist persons with disabilities with body activities. Several researches have been conducted on robotic orthoses: wearable orthoses for grasping assistance in activities of daily living (ADL) [8] and cylindrical grasping assistance [9]. A key technology in the development of a robotic orthosis is the ability to reflect the user's intention when assisting the user with the performance of motion. Bio-signal interface using electroencephalogram (EEG) [10] or electromyogram (EMG) [11] has been proposed. It enables the user him/herself to control the motion of the robotic orthosis. Recent research has attempted to apply robotic orthoses to rehabilitation therapy. However, in order to use these devices for rehabilitation therapy, the mechanism should be light and available to provide assistance with the motions required for ADL. Furthermore, it should be possible to perform rehabilitation exercise concurrent with ADL so as to enhance the therapeutic effects of the exercise.

It has been reported that mirrored image motion of the normal limb part is effective in functional recovery of the abnormal part [12]. This is called *mirror therapy*. If a robotic orthosis is capable of rehabilitation exercises such as those

J.H. Bae is with the Department of Mechatronics Engineering, Dong-Eui University, Busan, Korea (e-mail: jhbae@arms.deu.ac.kr).

Y.M. Kim was with Dong-Eui University, Busan, Korea. He is now with Heelnix Co., Busan, Korea (e-mail: ymkim@arms.deu.ac.kr).

I. Moon is with the Department of Mechatronics Engineering, Busan, Korea (phone: +82-51-890-2261; fax: +82-51-890-2883; e-mail: ihmoon@deu.ac.kr).

performed in mirror therapy, it would be useful in upper-limb rehabilitation. Our group originally proposed a wearable upper-limb rehabilitation device, called DULEX, which has 3 DOF for the motions of the wrist, the index finger, and a mechanism enclosing the other three fingers, but excluding the thumb [13]. The motion trajectory of DULEX was aligned to the user's hand motion through a parallel mechanism, and it was actuated by three pneumatic muscles. Because the pneumatic muscle was lighter than the electric motor, we were able to reduce the total weight of the device. However, the pneumatic muscle force was uni-directional, making DULEX only applicable in stretching exercises.

In this paper, we propose a wearable hand rehabilitation robot, called DULEX-II, capable of hand function assistance in stroke survivors (see Fig. 1). The basic purpose of DULEX-II is performing hand exercises to gradually increase range of motion (ROM) in the finger and wrist joints. Moreover, it can operate as a robotic orthosis capable of hand function assistance. In the mechanism design, we introduced the robotic orthosis concept of DULEX-II, using three linear actuators: a double-acting pneumatic cylinder for the wrist and two small-sized electric linear motors for the fingers. All mechanisms were analyzed by kinematics, and a control system for hand rehabilitation was then designed. The mechatronic properties of the device, including the control system, were tested in the basic experiments. From a series of experiments involving self-motion control using a data-glove worn as a normal limb part, we verified the possibility of applying DULEX-II as a hand rehabilitation robot with robotic orthosis function.

II. MECHANISM DESIGN

We used a double-acting pneumatic cylinder and two linear motors for DULEX-II, instead of the pneumatic muscles used in DULEX [13]. The design concept is basically the same, except that some parts are connected to actuators. The DULEX-II mechanism was designed based on kinematics analysis. The specifications for each part, such as ROM and maximum positions, are shown in Table 1.

TABLE I.   SPECIFICATIONS OF PARTS [DEGREE]

Items	Parts		
	distal-middle	proximal	wrist
maximum position	90	60	48
minimum position	0	-30	-42
range of motion	90	90	90

A. Design of Wrist Mechanism

Figure 2 shows the design model for the wrist mechanism, which is composed of 3-bar links. The wrist angle θ_w is controlled by the length of the piston rod in the pneumatic cylinder. This relation is expressed by the following equation:
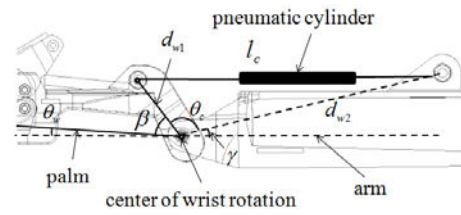
Fig. 2. Kinematics analysis model for the wrist mechanism.
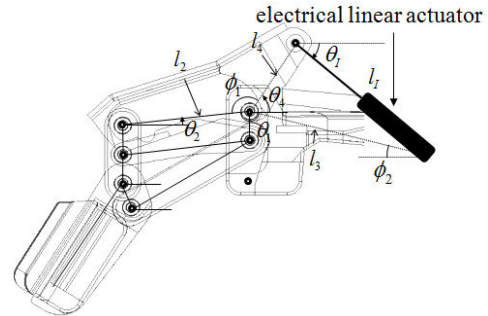
Fig. 3. Kinematics analysis model for the finger mechanism.

$$\theta_w = \beta + \cos\left(\frac{d_{w1}^2 + d_{w2}^2 - l_c^2}{2 d_{w1} d_{w2}}\right) + \gamma - \pi \tag{1}$$

Here, angles β and γ were the design variables. However, angle β was set to $60°$, considering the relations of force transfer. Then, we found the optimal solution to satisfy the relation between l_c and θ_w. The range of motion of the piston rod of the pneumatic cylinder, l_c, was 50 mm; the maximum and the minimum lengths, including the whole body of the cylinder, were 233 mm and 183 mm, respectively. The wrist angle θ_w was set to Table 1. The optimal solutions for d_{w1}, d_{w2}, and γ were 43.9 mm, 191.2 mm, and $14°$, respectively.

B. Design of Finger Mechanism

The finger mechanism of DULEX-II was designed using a parallel mechanism [13]. The proximal phalange and distal-middle phalange are operated by one linear motor (see Fig. 3). The ROM for the two phalanges is $90°$. The relation between the length of the motor, l_I, and the angle of the proximal phalange θ_2 is defined by the following equation:

$$\theta_2 = \pi - \left(\phi_1 + \cos^{-1}\left(\frac{l_3^2 + l_4^2 - l_I^2}{2 l_3^2 l_4^2}\right)\right) + \phi_2 \tag{2}$$

In the above equation, the lengths l_3 and l_4 and the angles ϕ_1 and ϕ_2 are the design variables related to θ_2 that is connected to the 3-bar link. The maximum and the minimum lengths of the linear motor are 62 mm and 42 mm, respectively. We then obtained the optimal solutions by using the length of the actuator and the predetermined maximum and minimum positions of θ_2 shown in Table 1. As a result,
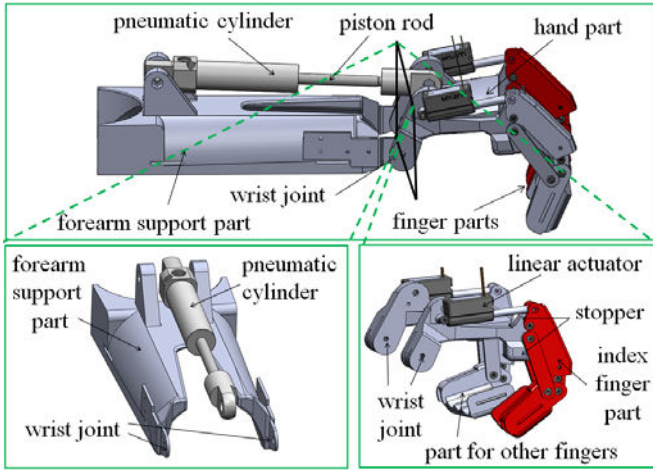
Fig. 4. 3D model of DULEX-II.

ϕ_1, ϕ_2, l_3, and l_4 were obtained as 129.8°, 10.6°, 53.5 mm, and 14.1 mm, respectively.

C. Design of DULEX-II

We designed a 3D model of DULEX-II using the design variables obtained in the above subsections (see Fig. 4). The pneumatic cylinder is fixed on the forearm part so that the hand part, including the finger parts, can be rotated on the wrist joint. Then, the movement of the piston rod generates wrist extension and flexion motions. The prototype DULEX-II is shown in Fig. 1. Its total weight is 504 g, including all actuators. Because the pneumatic cylinder and the electric linear motor can generate a steady force, DULEX-II can assist hand functions as well as hand rehabilitation. The piston rod of the pneumatic cylinder is actuated by a pressure difference in the cylinder; the stroke length is 50 mm and the maximum possible pressure is 1 MPa. However, the pneumatic cylinder has no sensor to measure the position of the piston rod, so an external linear potentiometer to measure the position is needed. The specifications of the electric linear motor attached to the finger mechanism are as follows: the weight is 19 g, the stroke length is 20 mm, and the maximum force is 18 N. Although the motor is small in size, a linear potentiometer is embedded in it.

III. DESIGN OF THE CONTROL SYSTEM

We designed a control system for wrist and finger mechanism movement. Figure 5 shows the pressure control system for the double-acting pneumatic cylinder. In Fig. 5, the inflow and outflow pressures of the cylinder are controlled by a one-way inflow valve. The inner pressure of the cylinder is measured by a pressure sensor. An air compressor supplies the air pressure, which is limited by a flow control valve. The piston rod of the cylinder is actuated by the pressure difference between the inner pressures, and the rod position is measured by a linear potentiometer attached in parallel to the cylinder. A motor control circuit to drive the electric linear motors was also designed.
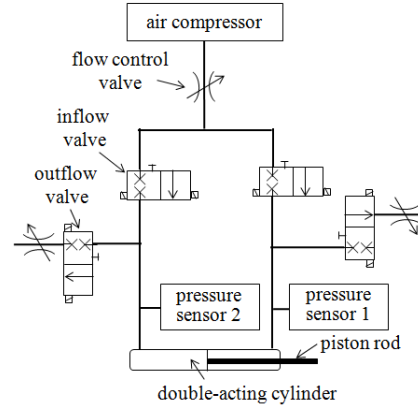
Fig. 5. Pressure control system for the double-acting cylinder.
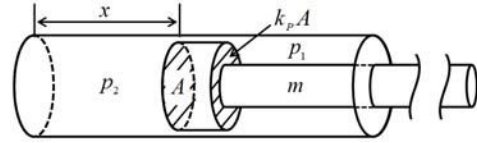
Fig. 6. Pneumatic cylinder actuator model.

A. Modeling of the Double-acting Pneumatic Cylinder

A cylinder actuation model was needed for the design of the wrist angle controller. Figure 6 shows the pneumatic cylinder actuator model. The position of the piston rod, x, is changed by the pressure difference in the cylinder. Its dynamics is expressed by the following equation:

$$m\frac{d^2x(t)}{dt^2} + b\frac{dx(t)}{dt} = A\left(-k_P p_1(t) + p_2(t)\right) \tag{9}$$

In Eq. (9), m is the mass of the piston rod, b is the coefficient of friction, and p_1 and p_2 represent the pressure in the cylinder. A in the right term means the left side area of the piston in the cylinder, and $k_P A$ is the right side area of the piston. Here, k_P is 0.84 because the left side area is reduced by the piston rod. To make Eq. (9) applicable to one input system, we set p_1 and p_2 to the following pressure values according to the control input u_P.

$$u_P(t) \le 0 \quad \begin{cases} p_1(t) = p_F \\ p_2(t) = k_P\left(p_F + u_P(t)\right) \end{cases} \tag{10}$$

$$u_P(t) > 0 \quad \begin{cases} p_1(t) = p_F - u_P(t) \\ p_2(t) = k_P p_F \end{cases} \tag{11}$$

In the above equations, p_F is the predetermined pressure of 3.1 kgf/cm^2. Then, Eq. (9) can be rewritten as follows:

$$m\frac{d^2x(t)}{dt^2} + b\frac{dx(t)}{dt} = Ak_P u_P(t) \tag{12}$$
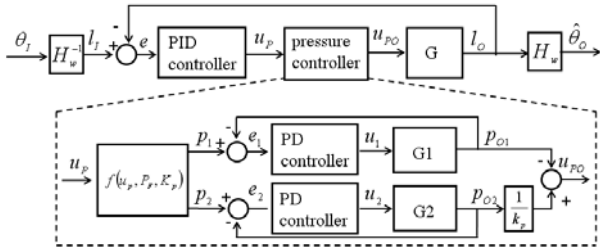
Fig. 7. Block diagram for the wrist controller.
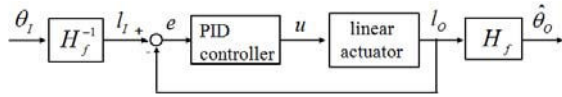
Fig. 8. Block diagram for the finger controller.

Consequently, the system transfer function can be obtained as follows:

$$\frac{X(s)}{U_P(s)} = \frac{k_p \alpha}{s(s + \beta)} \qquad (13)$$

where $\alpha = A/m$ and $\beta = b/m$, which were obtained by the system identification method, based on the experiments.

The inner pressure of the cylinder is determined by input flow control. We experimentally developed a PD controller without a pressure model by input flow.

B. Design of the Wrist Controller

The position controller for the wrist angle control was designed using the kinematic analysis in section II. Figure 7 shows the block diagram for the wrist controller. The inverse kinematics of the wrist mechanism, H_w^{-1}, first calculates the goal position of piston rod l_I from the goal angle of the wrist, θ_I. The output wrist angle can be estimated from the rod position l_o. A PID controller generates the control input u_P, and then the pressure inputs p_1 and p_2 are obtained through Eq. (10) and Eq. (11). The transfer function, G, is the same as Eq. (13), and its control input for position control, u_{PO}, is the pressure difference, expressed by the following equation:

$$u_{PO} = -P_{O1} + \frac{1}{k_p} P_{O2} \qquad (14)$$

C. Design of the Finger Controller

Using the kinematics analysis of the finger mechanism shown in section II, we designed a PID controller for finger position control. In Fig. 8, H_f^{-1} is the inverse kinematics of the finger mechanism, and the finger flexion angle is estimated from the linear motor length.

IV. EXPERIMENTAL RESULTS

The performances of the developed controllers were experimentally evaluated (see Fig. 9). The maximum pressure
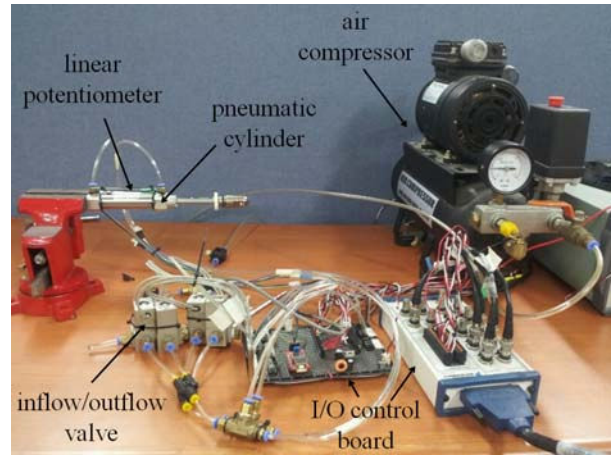
Fig. 9. Experimental setup for controller evaluation.

of the air compressor was set to $3.3\,\text{kgf/cm}^2$. The designed PD controller in Fig. 7 works at every 10msec cycle.

Figure 10 shows the basic experimental results. The first graph shows the position control result; the dotted line is the goal position and the solid line is the control result. The second graph shows the measured pressure in the cylinder. The last graph is the valve control data: I, S, and O mean inflow valve on, stop for both valves, and outflow valve on, respectively. The pressure was $p_1 = 3.1$ kgf/cm^2 and $p_2 = 2.6$ kgf/cm^2. When the goal position was increased to 40 mm at 4 seconds, the pressure p_1 was reduced, but the pressure p_2 was maintained. After 5 seconds, the piston rod reached the goal position, and the cylinder pressure was held at the initial pressure to maintain a state of equilibrium. The maximum control error was less than 0.5 mm.

The finger controller was also tested. Figure 11 shows the test results; the dotted line is the goal position, and the solid line is the controlled position. In the results, even though no overshoot was shown in the position control result, a 0.1 mm error occurred when the length of the linear motor was changed from 2.5 mm to 12.5 mm at the goal position. The error caused a finger angle error of about 0.45 degrees, but this did not present a significant problem during user rehabilitation exercises.

Experiments related to self-motion control using a data-glove were also performed. The experimental setup is shown in Fig. 12. A healthy man was used as the experimental subject; we assumed that his right hand was normal and that his left hand was the disabled limb requiring rehabilitation therapy. Therefore, the subject wore a data-glove on his right hand and the DULEX-II on the left hand, as shown in Fig. 12. First, motion commands were given by the data-glove. We measured the angles of the wrist, the index finger, and the middle finger from the data-glove output. Then the goal positions of each actuator were calculated by the inverse kinematics obtained in section II. Finally, the actuators were controlled using the control algorithm shown in section III.
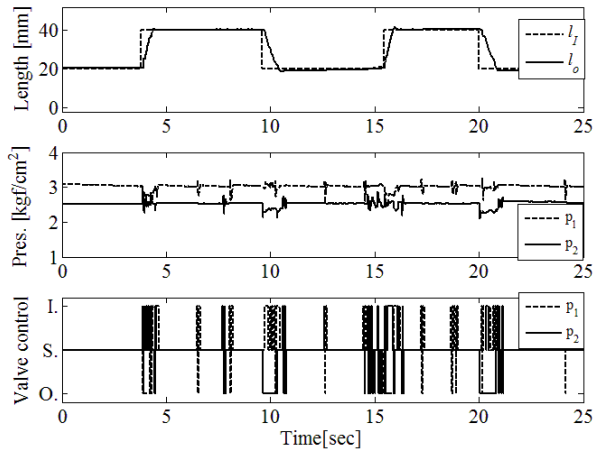
Fig. 10. Results of the basic experiments.
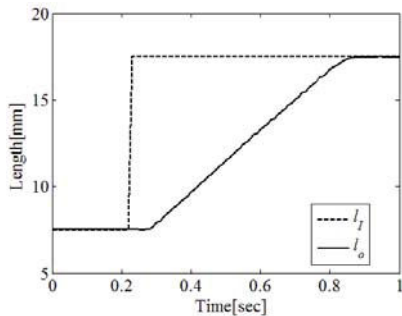
Fig. 11. Result for the finger position control.

Fig. 12. Experimental setup to test self-motion control.

Fig. 13. Experimental results for self-motion control.
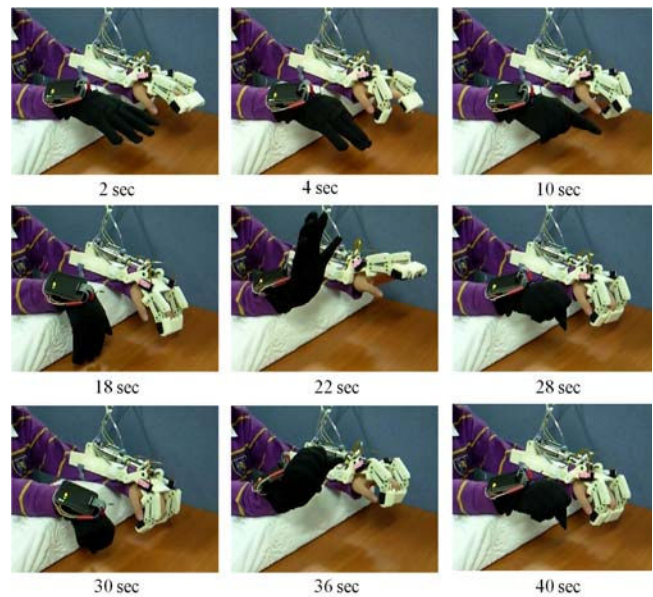
Fig. 14. Corresponding motion sequences to the experimental results shown in Fig. 13.

Figure 13 shows the experimental results of the self-motion control test. The dotted lines in the graph show the goal position given by the data-glove, and the solid lines show the position control results. In the experiment, we asked the subject to perform eight different motions. The initial state was the stretched posture, as shown in Fig.14, at 2 seconds. The first event was flexion of the index finger at 3 seconds, and then the index finger of the DULEX-II was flexed. The corresponding sequence is shown in Fig. 14 at 4 seconds. At 15 seconds, the wrist flexion command was given, and DULEX-II was also controlled, as shown in Fig. 14 at 18 seconds. At 22 seconds, the wrist was extended. The time delay in the motor linear control was about 1 second, but this did not pose a problem in the performance of the rehabilitation exercise. The experiments proved that the use of DULEX-II is feasible in hand rehabilitation, and that it is capable of assisting with hand functions.

V. CONCLUSIONS

In this paper, we proposed a hand rehabilitation robot, DULEX-II, for application in stroke survivor therapy exercises. To overcome problems with the original DULEX [13], we introduced linear actuators, such as a double-acting pneumatic cylinder and a linear electric motor, to the mechanism design. A control system for the actuators was also proposed and experimentally evaluated. From the basic experimental results, we determined that the pneumatic cylinder and the linear motor were controlled under 0.5 mm and 0.1 mm error, respectively. The self-motion control results also demonstrated DULEX-II's capability to assist with hand functions.

When a patient performs rehabilitation exercises, spasm often occurs. Thus, it is important to prevent additional muscular injuries in rehabilitation exercise. Bio-feedback control is a pertinent issue, and will be studied in future work.

REFERENCES

[1] V. Feigin, "Stroke epidemiology in the developing world," *The Lancet*, vol. 365, issue 9478, pp. 2160-2161, 2005.

[2] J. C. Perry, J. Rosen and S. Bums, "Upper-limb powered exoskeleton design," *IEEE Trans. on Mechatronics*, vol. 12, no. 4, pp. 408-417, 2007.

[3] D. E. Barkana, F. Wang, J. Das, N. Sarkar and T. E. Groomes, "A step toward increasing automation in robot-assisted rehabilitation," in *Proc. IEEE Conf. on Biomedical Robotics and Biomechatronics*, pp. 930-935, 2008.

[4] T. G. Sugar, E. J. Koeneman, J. B. Koeneman, R. Hernam, H. Huang, R. S. Schultz, D. E. Herring, J. Wanberg, S. Balasubramanian, P. Swenson and J. A. Ward, "Design and control of RUPERT: a device for robotic upper extremity repetitive therapy," *IEEE Trans. on Neural Systems and Rehabilitation Engineering*, vol. 15, no. 3, pp. 336-346, 2007.

[5] E. J. Koeneman, R. S. Shultz, S. L. Wolf, D. E. Herring and J. B. Koeneman, "A pneumatic muscle hand therapy device," in *Proc. IEEE Conf. on Medicine and Biology Society*, San Francisco, 2004, pp. 2711-2713.

[6] S. Ueki, H. Kawasaki, S. Ito, Y. Nishimoto, M. Abe, T. Aoki, Y. Ishiguro, T. Ojika and T. Mouri, "Development of a hand-assist robot with multi-degree-of-freedom for rehabilitation therapy," *IEEE/ASME Trans. on Mechatronics*, vol. 17, no. 1, pp. 136-146, 2012.

[7] M. Hioki, H. Kawasaki, H. Sakaeda, Y. Nishimoto and T. Mouri, "Finger rehabilitation system using multi-fingered haptic interface robot controlled by surface electromyogram," in *Proc. of the 2010 3rd IEEE RAS & EMBS*, Tokyo, 2010, pp. 276-281.

[8] Y. Hasegawa, Y. Mikami, K. Watanabe, Z. Firouzimehr and Y. Sankai, "Wearable handing support system for paralyzed patient," in *Proc. 2008 IEEE/RSJ International Conf. on Intelligent Robots and Systems*, Nice, 2008, pp.741-746.

[9] T. M. W. Burton, R. Vaidyanathan, S. C. Burgess, A. J. Turton and C. Melhuish, "Development of a parametric kinematic model of the human hand and a novel robotic exoskeleton," in *Proc. 2011 IEEE International Conf. on Rehabilitation Robotics*, Zurich, 2011, pp. 172-178.

[10] R. Ortner, B. Z. Allison, G. Korisek, H. Gaggl, and G. Pfurtscheller, "An SSVEP BCI to control a hand orthosis for persons with tetraplegia," *IEEE Trans on Neural Systems and Rehabilitation Engineering*, vol. 19, no. 1, 2011.

[11] J. Stein, K. Narendran, J. McBean, K. Krebs and R. Hughes, "Electromyography-controlled exoskeletal upper-limb-powered orthosis for exercise training after stroke," *American J. of Physical Medicine & Rehabilitation*, vol. 86, no.4, pp. 255-261, April 2007.

[12] S. Sütbeyaz, G. Yavuzer, N. Sezer and B. F. Koseoglu, "Mirror therapy enhances lower-extremity motor recovery and motor functioning after stroke: a randomized controlled trial," *Archives of Physical Medicine and Rehabilitation*, vol. 88, no. 5, pp. 555-559, 2007.

[13] Y. M. Kim and I. Moon, "Development of a wearable hand rehabilitation device for stroke patients," in *Proc. International Conf. on Biomedical Engineering*, Innsbruck, 2010, track 680-155.